Properties of Nonlocal Pseudopotentials of Si and Ge Optimized under Full Interdependence among Potential Parameters

Bull. Coll. Med. Sci. Tohoku Univ. 2(1) : 7~16, 1993

Properties of Nonlocal Pseudopotentials of Si and Ge Optimized under Full Interdependence among Potential Parameters

Teiji KOBAYASI and Hisashi NARA*

General Education, College of Medical Sciences, Tohoku University
**Education Center for Information Processing, Tohoku University*

十分なポテンシャルパラメタ間相互依存性下で最適化した Si, Ge 半導体の非局所擬ポテンシャルの性質

小林悌二, 奈良　久*

東北大学医療技術短期大学部　一般教育
*東北大学情報処理教育センター

Key words: Empirical pseudopotential, Nonlocal potential, Silicon, Germanium, Energy band structure

Empirical nonlocal pseudopotentials of Si and Ge which can describe the electronic energy structure over a wide energy range of more than 20 eV from the bottom of the valence band have been determined. The nonlocality of the potential is described by the Heine-Abarenkov or the Gaussian model with the angular-momentum (l) dependent parameters of core radius R_l and potential depth or height A_l. The local-part parameters are the usual form factors. These parameters are optimized interdependently using the nonlinear least squares method so as to reproduce various energy level spacings obtained experimentally. The result shows: (1) Keeping an effective "volume" $A_l R_l^{2l+3}$ of the potential within a "physical" range, the optimized R_l and A_l can reproduce the same electronic structure over their wide ranges, as if they are not confined in their literal meanings. This means that the potential volume is a more significant parameter than the individual A_l or R_l. (2) A parameter-interdependence is essential for a fine description of a wide-energy-range electronic structure. (3) The optimized nonlocal pseudopotentials reproduce the energy band structure within the deviations of 2.9% for Ge and of 3.8% for Si.

The importance of a full parameter-interdependence in a wide-energy-range fitting and the properties of the potentials are discussed.

Introduction

The empirical pseudopotential (EPP) method[1)~3)] has proven a powerful tool for understanding electronic energy band structure (EBS) of semiconductors. The main sources of experimental input to determine the EPP were previously the optical absorption data, and the main interest was in describing the EBS near the band gap. Now the X-ray[4)~6)] and ultra-

violet[7)8)] photoemission spectroscopies (XPS and UPS) provide us information about the EBS away from the band gap, and the Schottky barrier electroreflectance technique[9)~11)] has been providing very precise values for the interband energy level spacing (LS) in the optical region. These data are related to the electronic energy states in the whole valence band and in the conduction band more than 10 eV above the band gap.

In the EPP composed of a small number of parameters consistent with the EBS over such a wide range, the parameters should be determined to be fully interdependent among themselves. Since the availability of these data, several authors[12)~18)] attempted to understand the EBS of semiconductors in a wider energy range. Cohen and his coworkers[12)~16)] determined the nonlocal EPP's (NLEPP) of many semiconductors by calculating the valence band density of states to give a good fit to the XPS data. The NLEPP's of Ge and GaAs were detremined by Phillips and Pandey[18)]. In their pioneer works, however, it seems to be not necessarily clear how the parameters are determined interdependently and what criteria are adopted for the quality of overall fitness. Some of the parameters were fixed *a priori* or chosen to be common to materials. Since the parameters for nonlocality were connected to a particular structure in the density of states, and were determined in a very complex way, it seems to be difficult to determine them in a fully interdependent way with the other parameters.

It may be supposed that many Fourier components of EPP are necessary for a description of EBS in a wide energy range. On the contrary, the following Kane's viewpoint has been widely accepted. Adopting the Heine-Abarenkov potential[19)], Kane[20)] investigated the EBS of Si to fit the indirect band gap and the valence- and the conduction-band cycrotron resonance mass constants. He showed that higher Fourier components of the EPP were nearly linearly dependent in their effects on the EBS parameters he investigated, and that only the three lower components $V(\boldsymbol{k}, \boldsymbol{k}+\boldsymbol{G})$ with the reciprocal lattice vectors $\boldsymbol{G}$ of $\boldsymbol{G}^2=3$, 8 and 11 [in units of $(2\pi/a)^2$, where a is the lattice constant] were essential. It should be noted, however, that such a lower potential-truncation cannot be justified unless the EPP components are determined under a full parameter-interdependence. The following is an example showing the significance of the parameter-interdependence. The Kane's adjustable factor $F(\boldsymbol{G})$ for $V(\boldsymbol{k}, \boldsymbol{k}+\boldsymbol{G})$ are chosen to be common to $V(\boldsymbol{k}, \boldsymbol{k}+\boldsymbol{G})$ with $\boldsymbol{G}^2 \geqq 19$. Thus the possibility of the interdependent modulation among the components with $G^2=16, 19$ and 24, which affect higher energy states around the $\Gamma_{12'}$ state lying 8~9 eV above the valence-band top, suffers a serious restriction. In fact, the largest error (~56%) was in the valence-band mass constant[20)] mainly originating from the interaction of the valence-band top states with the $\Gamma_{12'}$ state. The large discrepancy is unnatural considering that the errors were ~10% in the indirect gap and only a few percents in the other EBS parameters.

The purpose of this paper is to discuss the properties of EPP determined in a fully interdependent way and of the corresponding EBS in detail. We determine the EPP parameters by the nonlinear least squares method, in which all of the parameters are simultaneously optimized under a definite criterion of minimizing the root-mean-square (*rms*) deviation. The optical, UPS and XPS data are used. We obtain the NLEPP's of Si and Ge which can describe the EBS over a range of more than 20 eV from

the valence-band bottom. The outline of the method is previously described[21]. Some details are given in the next section for discussion that follows. The EPP's of Si and Ge determined are given in the third section. The final section is devoted to discussion of the properties of the NLEPP and the EBS from the viewpoint of the interdependent modulation of parameters.

Method of Optimization of EPP Parameters

Let us define our EPP of a semiconductor as a superposition of the pseudo-atomic potential of the form $V(\boldsymbol{r})=V_{\mathrm{L}}(\boldsymbol{r})+V_{\mathrm{NL}}(\boldsymbol{r})$, where V_{L} and V_{NL} are local and nonlocal parts, respectively. The angular-momentum (l) dependent nonlocal part is written as $V_{\mathrm{NL}}(\boldsymbol{r})=\sum_l v_l(r)\sum_m |Y_{lm}><Y_{lm}|$, where Y_{lm} is the spherical harmonics. For the radial part $v_l(r)$ we chose either a square-well form of Heine-Abarenkov[19] type

$$v_l(r)=A_l\Theta(R_l-r), \tag{1}$$

or a Gaussian well form[16]

$$v_l(r)=A_l\exp[-r^2/R_l^2], \tag{2}$$

where $\Theta(x)=1$ for $x\geqq 0$, and $=0$ for $x<0$. We regard the Fourier components of $V_{\mathrm{L}}(\boldsymbol{r})$ as the EPP local parameters and the well-depth or height A_l and the cut-off radius R_l as the nonlocal ones.

Our nonlinear least squares method requires that the *rms*-deviation of the calculated LS's from the experimental ones defined by

$$\delta=[\sum_{(i,j)}^{m}\{\Delta E^{(i,j)}\}^2/(m-N)]^{1/2} \tag{3}$$

should be minimum[21]. In eq. (3), $\Delta E^{(i,j)}=E_{\mathrm{exp}}^{(i,j)}-E_{\mathrm{calc}}^{(i,j)}$, where $E_{\mathrm{exp}}^{(i,j)}$ and $E_{\mathrm{calc}}^{(i,j)}$ are the observed and calculated LS's between the ith state at the wave vector $\boldsymbol{k}=\boldsymbol{k}_{\mathrm{I}}$ and jth at $\boldsymbol{k}=\boldsymbol{k}_{\mathrm{J}}$, respectively, in the m chosen pairs (i,j). N is the number of the EPP parameters.

The calculated energies given by solving the EPP secular equation depend nonlinearly on the EPP parameters. The starting values of the parameters are improved step by step by iterations untill δ is minimized. Let us denote the parameters by $P_\nu(\nu=1,2,\cdots,N)$ and write as $P_\nu(n+1)=P_\nu(n)+\Delta P_\nu$, where $P_\nu(n)$ is the value at the nth iteration. These corrections ΔP_ν are determined *simultaneously* by solving a system of linear equations[22]

$$\sum_{\nu=1}^{N}\{\sum_{(i,j)}^{m}(Q_\nu^i-Q_\nu^j)(Q_{\nu'}^i-Q_{\nu'}^j)\}\Delta P_\nu = \sum_{(i,j)}^{m}(E_{\mathrm{exp}}^{(i,j)}-E_{\mathrm{calc}}^{(i,j)}(n))(Q_{\nu'}^i-Q_{\nu'}^j) \tag{4}$$
$$(\nu'=1,2,\cdots,N),$$

where $E_{\mathrm{calc}}^{(i,j)}(n)$ is the value at the nth iteration, Q_ν^i is given by

$$Q_\nu^i=\sum_{q,q'}[C_q^i(\boldsymbol{k}_{\mathrm{I}})]^*(\partial H(\boldsymbol{k}_{\mathrm{I}})/\partial P_\nu)_{qq'}C_{q'}^i(\boldsymbol{k}_{\mathrm{I}}), \tag{5}$$

$H(\boldsymbol{k}_{\mathrm{I}})$ is the pseudo-Hamiltonian matrix at $\boldsymbol{k}=\boldsymbol{k}_{\mathrm{I}}$ in the plane wave (PW) representation, and the ith pseudo-wave function at $\boldsymbol{k}=\boldsymbol{k}_{\mathrm{I}}$ is expanded as $\Psi_{\boldsymbol{k}_{\mathrm{I}}}^i(\boldsymbol{r})=\sum_q C_q^i(\boldsymbol{k}_{\mathrm{I}})\exp[\mathrm{i}(\boldsymbol{k}_{\mathrm{I}}+\boldsymbol{K}_q)\cdot\boldsymbol{r}]$, $\boldsymbol{K}_q$ being the reciprocal lattice vector. Equation (4) shows that all of the parameters are determined automatically in an interdependent way. Among the parameters $V_l(\boldsymbol{K}_q^2)$, A_l and R_l, we vary the value of R_l externally in seeking a minimum of δ, because the accurate evaluation of $(\partial H(\boldsymbol{k}_{\mathrm{I}})/\partial P_\nu)_{qq'}$ is not practical for the parameter R_l in aspects of algorithm and computational accuracy.

A very small LS of the order of, for example, 0.1 eV could become serious. The small LS of $E(\Gamma_{2'})-E(\mathrm{L}_1)=+0.15$ eV[23][24] in Ge should be accurately reproduced to make sure that the conduction band minimum is certainly located at $\boldsymbol{k}=\mathrm{L}$, not at $\boldsymbol{k}=\Gamma$. The δ should be at least 0.1 eV or less, but it is not so expectable

because of a larger mean error in experiment. In such cases, the minimization under the relative deviation $\bar{\delta}$ defined by

$$\bar{\delta}=[\sum_{(i,j)}^{m}\{\overline{\Delta E}^{(i,j)}\}^2/(m-N)]^{1/2} \qquad (6)$$

is essential, where $\overline{\Delta E}^{(i,j)}=\Delta E^{(i,j)}/E_{\mathrm{exp}}^{(i,j)}$. The corrections $\Delta\bar{P}_\nu$ of the EPP parameters defined by $P_\nu(n+1)=P_\nu(n)+\Delta P_\nu=P_\nu(n)[1+\Delta\bar{P}_\nu]$ are obtained by solving eq. (4) under a slight modification in eq. (5).

The *rms*-deviation δ or $\bar{\delta}$ is a complicated function of the EPP parameters and the input LS's. It will be possible that we fall into a bottom of a wrong valley of δ ($\bar{\delta}$) in the multi-parameter-space depending on the starting parameter set. Examples of the multi-valley are shown later.

The psewdo-wave functions $\Psi_k^i(\boldsymbol{r})$ are calculated at each iteration using all the PW's with $\boldsymbol{K}_q$ satisfying $(\hbar^2/2m)[|\boldsymbol{k}+\boldsymbol{K}_q|^2-|\boldsymbol{k}|^2]\leqq E_{\max}$. A choice of $E_{\max}=14\sim22$ in units of $(\hbar^2/2m)(2\pi/a)^2$ turns out to be practical. In the actual calculation, $E_{\max}=14$ is adopted.

Empirical Pseudopotentials of Si and Ge

We determine the the EPP's of Si and Ge using the optical absorption data of the Shottky barrier electroreflectance spectroscopy[9)~11)], the XPS[4)~6)] and UPS[7)8)25)] data. For Ge, such a set of data was carefully selected by Phillips and Pandey[18)]. From these, we adopt only the data interconnecting the states at the high symmetry points Γ, X and L. The points of the less symmetry directions Δ and Σ are not convenient in the iteration process. For Si, we select the optical[9)~11)26)~29)], UPS[25)] and XPS[4)] data. The XPS data are re-expressed relative to the sharpest peak arising from the L_1 valence state[4)], not to the less accurate $\Gamma_{25'}$ edge. For both Si and Ge, the UPS[25)] data adds the information of the higher Γ_1 and $\Gamma_{12'}$ conduction states. Thus the energy range covers more than 20 eV from the valence-band bottom. The input data are listed in Tables II (Si) and III (Ge) [the superscripts v and c on the level notation (see Fig. 2) refer to the valence and the conduction bands, respectively].

Good starting values of the EPP parameters were carefully chosen by test-working with the smaller- to full-sized Hamiltonian matrices ($E_{\max}=8\sim14$). We were also guided by the existing parameter sets[1)~3)12)~18)20)]. Iteration convergence was exceedingly good. For example, only three or four iterations were enough, in the six-parameter-fit, to determine the parameters to four significant figures.

The results of NLEPP using the square-well form of eq. (1) and the local EPP (LEPP) are

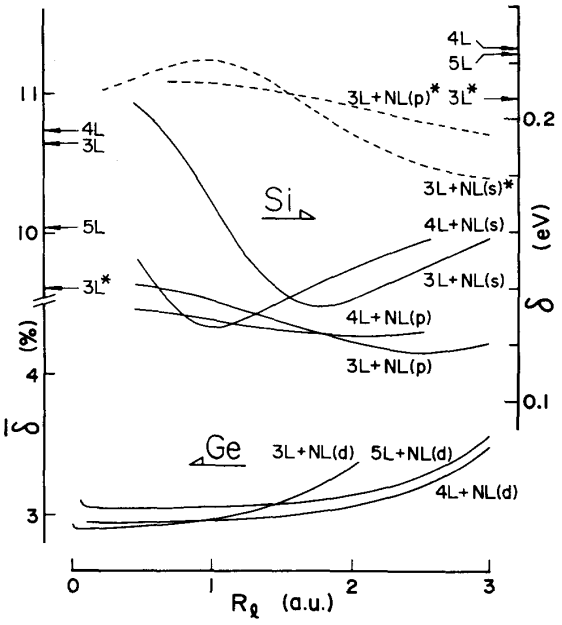

Fig. 1. The variation of the *rms*-deviation δ(Si) in eV and $\bar{\delta}$(Ge) in % as functions of the cut-off radius R_l, for the several nL+NL(l) EPP's. The results for the local fittings nL are indicated by the arrows. The dashed curves correspond to the higher minima of δ in the parameter space. For the meaning of the asterisked results, see text.

Table I. The empirical pseudopotential parameters, V_L (G^2), A_l (in Ry/atom) and R_l (in a.u.) determined for Si and Ge corresponding to the typical values of δ (Si) (in eV) and $\bar{\delta}$ (Ge) (in %). For the meaning of the asterisked results, see text.

		$V_L(3)$	$V_L(8)$	$V_L(11)$	$V_L(16)$	$V_L(19)$	A_0	A_1	A_2	R_l	δ(Si), $\bar{\delta}$(Ge)
	3L*	−0.2213	0.0529	0.0763							0.207 eV
	4L	−0.2082	0.0409	0.0835	0.0189						0.225
	5L	−0.2066	0.0269	0.1106	0.0247	0.0760					0.223
Si	3L+NL(s)	−0.2289	0.0191	0.0676			0.2391			1.75	0.134
	3L+NL(p)	−0.2021	0.0363	0.0769				−0.0604		2.5	0.117
	4L+NL(s)	−0.2631	−0.0262	0.0504	−0.0617		2.233			1.0	0.127
	4L+NL(p)	−0.2019	0.0332	0.0797	−0.0134			−0.1385		2.0	0.123
	3L*	−0.2852	0.0604	0.0173							9.61%
	3L	−0.2508	0.0257	0.0441							10.64
	4L	−0.2555	0.0363	0.0224	0.0627						10.73
	5L	−0.2440	−0.0139	0.0867	0.0181	0.1131					10.04
Ge	3L+NL(d)	−0.2425	0.0253	0.0529					4.892×10^{13}	0.02	2.89
	3L+NL(d)	−0.2422	0.0255	0.0526					83.77	0.98	2.96
	4L+NL(d)	−0.2437	0.0299	0.0432	0.0261				71.27	1.0	2.95
	5L+NL(d)	−0.2407	0.0223	0.0529	0.0140	0.0146			5.956×10^{8}	0.1	3.05
	5L+NL(d)	−0.2402	0.0223	0.0520	0.0184	0.0167			79.40	0.98	3.05

presented here. The Gaussian well model gave essentially the same results, which will be briefly shown later. We introduce the abbreviated notation of nL+NL (l), which means the optimization with the first n local parameters $\{V_L(\boldsymbol{G}_i^2),\ i=1, 2, \cdots, n\}$ and the nonlocal parameters (A_l, R_l). First, we discuss the R_l-dependence of δ and $\bar{\delta}$. Figure 1 shows the variations of the achieved δ for Si and $\bar{\delta}$ for Ge as functions of the cut-off radius R_l for the core repulsion. The results of the LEPP (nL) are indicated by the arrows. The pairs of the 3L+NL (l) and 3L+NL (l)* ($l=s$ or p) for Si and the 3L and 3L* for Ge represent the examples of the multiple minima of δ ($\bar{\delta}$) in the parameter space (for the meaning of the asterisked results, see the fourth section). The typical EPP parameters obtained are listed in Table I. An excellent capability of the interdependent change among the parameters appears typically in the example of the 4L+NL (s) fitting for Si: The identical results were obtained after only a few iterations even if the starting parameters were of the 4L or the 3L+NL (s) type. From Fig. 1 and Table I, the following observations can be made: (a) The achieved values of δ ($\bar{\delta}$) are successfully small. (b) The R_l-dependence of the δ ($\bar{\delta}$) is rather weak. (c) For both Si and Ge, the NLEPP fittings improves the fits substantially over the LEPP fittings. (d) For Ge, the minima of $\bar{\delta}$ occur at the extremely small values of $R_2\cong0.02$ atomic units (a.u.) in 3L+NL (d) and 0.1 a.u. in 5L+NL (d). For Si, the minimum in 3L+NL (p) occurs at $R_1=2.5$ a.u., which exceeds half of the Si-Si bond length. These values may seem curious for the core radii. (e) The qualities of the fitness under the various potential-truncations, namely the 3L, 3L+NL (s and p), 4L+NL (s and p) for Si and the (3, 4 and 5) L+NL (d) for Ge, are almost the same over a certain range of R_l.

Discussion

We discuss the properties of the optimized EPP's giving the characteristic observations (a) ~(e) and of the corresponding EBS from the

viewpoints of the potential nonlocality and the interdependent modulation. The EBS's of Si and Ge calculated with the typical 3L+NL (p) (R_1=2.5 a.u.) and 3L+NL (d) (R_2=0.98 a.u.) EPP are shown in Fig. 2 (A) and (B), respectively.

As described in the observation (d), the value of our R_l is not necessarily confined in the range of the physical core radius. This may seem curious, but is understandable from the two facts: (1) Physically, an electron does not feel the potential strength A_l itself, but does a "volume" of the potential; $A_l R_l^{2l+3}$. (2) The volume is very weakly R_l-dependent keeping a "physical" value, through the R_l-dependently optimized A_l. This is the base of the observation (b).

Detailed comparison of the calculated LS's with the experimental ones is given in Table II for Si and in Table III for Ge. The experimental LS's adopted as the input data are compared in the upper parts of the tables. In the lower parts the other LS's for which the experimental data are available are compared. The results of Tables II and III indicate clearly that, for both Si and Ge, the nonlocality of the EPP is essential in describing the EBS over the wide energy range of our interest [the observation (c)]. As seen from $E(\Gamma_{2'})-E(\Gamma_{25'})$[23] and $E(L_1)-E(\Gamma_{25'})$[24] in Table III, the very small LS $E(\Gamma_{2'})-E(L_1)=+0.15$ eV in Ge is satisfactorily accounted for in all of the NLEPP fittings (0.13 ~0.14 eV), compared with the values of −0.07 (3L*), +0.09 (3L) and +0.13 (5L) eV in the LEPP fittings. The large discrepancies in the higher-lying Γ_1 and $\Gamma_{12'}$ conduction states in the LEPP

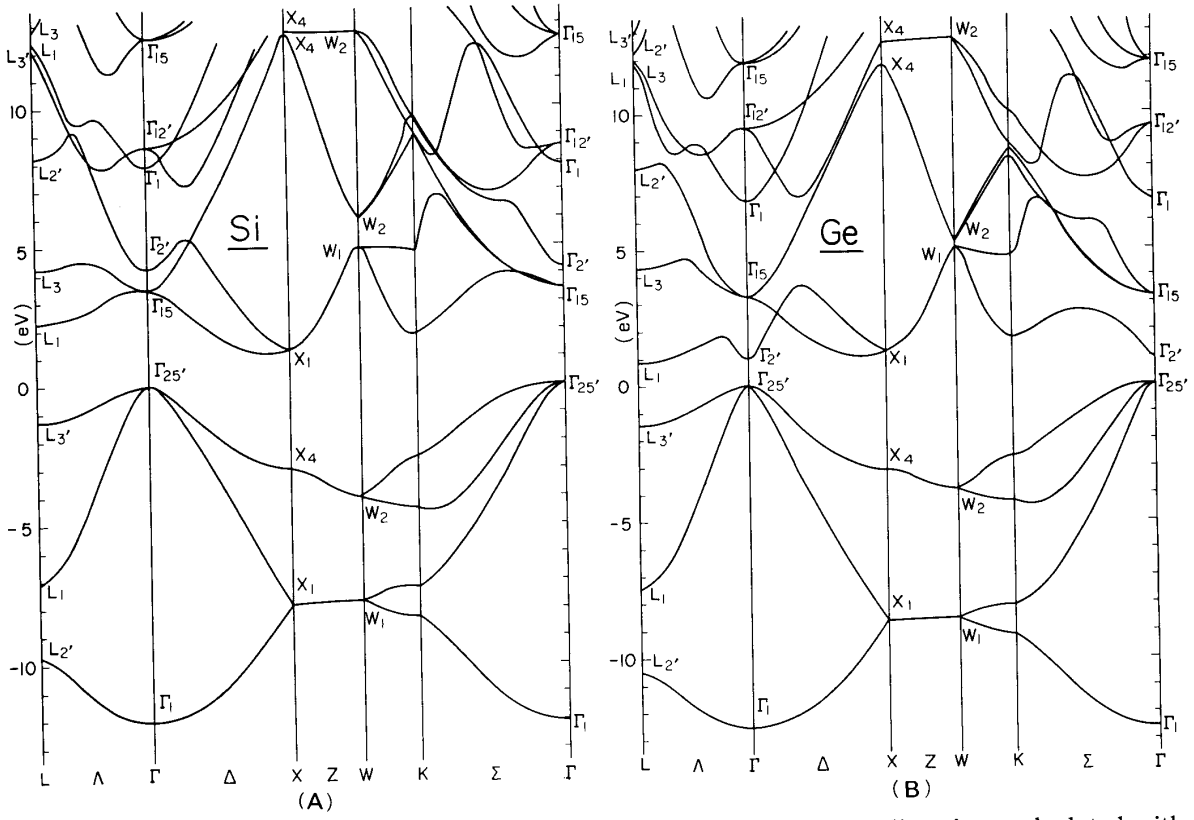

Fig. 2. (A) The energy band structure of Si along the principal symmetry directions calculated with the 3L+NL(p) EPP at R_1=2.5a.u. given in Table I and (B) of Ge calculated with the 3L+NL (d) EPP at R_2=0.98 a.u. The energy is in units of eV.

Table II. Comparison of the calculated LS's (in eV) of Si with experiment. In the upper part of the table, the comparison with the experimental LS's adopted as the input data for determining the EPP is made. In the lower part the comparison with the other experimental data available is added.

	(i, j)	$E_{\mathrm{exp}}^{(i,j)}$	3L*	5L	3L+NL(s) $R_0=1.75$	3L+NL(p) $R_1=2.5$	4L+NL(s) $R_0=1.0$	4L+NL(p) $R_1=2.0$a.u.
Optical	$\Gamma_{15}^{c}-\Gamma_{25'}^{v}$	3.40[27]	3.40	3.37	3.50	3.46	3.41	3.47
	$\Gamma_{2'}^{c}-\Gamma_{25'}^{v}$	4.20[26]	4.30	4.31	4.13	4.21	4.22	4.19
	$X_1^{c}-X_4^{v}$	4.20[29]	4.19	4.08	4.09	4.20	4.15	4.20
	$L_1^{c}-L_3^{v'}$	3.45[27][29]	3.40	3.38	3.34	3.45	3.42	3.46
	$L_3^{c}-L_3^{v'}$	5.50[27]	5.22	5.51	5.40	5.45	5.49	5.46
	$X_1^{c}-\Gamma_{25'}^{v}$	1.20 §	1.16	1.15	1.15	1.09	1.20	1.13
XPS	$L_1^{v}-L_2^{v'}$	2.6 ¶	2.91	2.92	2.64	2.57	2.61	2.57
	$X_4^{v}-L_1^{v}$	4.4 ¶	4.32	4.39	4.20	4.23	4.17	4.19
	$W_2^{v}-L_1^{v}$	3.0 ¶	3.35	3.40	3.21	3.31	3.19	3.19
UPS	$\Gamma_1^{c}-\Gamma_{25'}^{v}$	7.6[25]	8.32	7.63	7.63	7.64	7.60	7.61
	$\Gamma_{12'}^{c}-\Gamma_{25'}^{v}$	8.3[25]	7.76	8.28	8.35	8.35	8.30	8.30
	δ (eV)		0.207†	0.223	0.134	0.117	0.127	0.123
	$\Gamma_{25'}^{v}-\Gamma_1^{v}$	12.4±0.6[7] 14.7[4]	12.63	12.54	12.47	12.28	12.13	12.22
	$\Gamma_{25'}^{v}-\Sigma_{\mathrm{min}}^{v}$	4.4±0.2[7] 4.7[4]	4.55	4.46	4.50	4.70	4.50	4.47
	$\Gamma_{25'}^{v}-W_1^{v}$	7.8[4]	8.19	8.16	7.79	7.92	7.74	7.84
	$\Gamma_{25'}^{v}-L_2^{v'}$	9.2[4]	10.27	10.23	9.79	9.91	9.73	9.84
	$\Gamma_{25'}^{v}-W_2^{v}$	3.6[4]	4.01	3.92	3.94	4.13	3.93	4.07
	$\Gamma_{25'}^{v}-L_1^{v}$	6.4±0.4[7] 6.6[4]	7.36	7.32	7.15	7.34	7.12	7.26
	$\Sigma_3^{c}-\Sigma_2^{v}$	4.44[27]	4.25	4.16	4.19	4.27	4.21	4.27
	$\Delta_{\mathrm{min}}^{c}-\Gamma_{25'}^{v}$	1.15§	1.04	1.00	1.01	0.96	1.06	1.00

† Value estimated by assuming that the calculated values of 7.76eV and 8.32eV correspond to the experimental values of 7.6eV and 8.3eV, respectively.

§ Estimated from the data for $\Delta_{\mathrm{min}}-\Gamma_{25'}=1.15$eV (ref. 28).

¶ Re-expressed data of ref. 4 relative to the sharpest L_1 peak (see text).

fittings are also removed perfectly. Let us consider the level order of the two states. In Si, in all fittings except for the 3L, the upper 3L+NL (s) and 3L+NL (p) ones (the dashed curves in Fig. 1), we have the $\Gamma_{12'}$ level lying above the Γ_1 level; $\Delta E=E(\Gamma_{12'})-E(\Gamma_1)>0$. The fittings giving $\Delta E<0$ are asterisked in Fig. 1. In many trials for Si, a set of 3L EPP parameters giving $\Delta E>0$ was not found. In the 3L*, 3L+NL (s)* and 3L+NL (p)* fittings, $|\Delta E|$'s are 0.5~0.6 eV, which are smaller than the observed 0.7 eV[25]. The situation is well improved in the 4L, 5L and the (3 and 4)L+NL (s and p) fittings. In particular, it is completely reproduced at the minimum δ in every NLEPP fitting (0.69~0.72 eV, Table II). In the LEPP fitting for Ge, we have both cases of $\Delta E>0$ and $\Delta E<0$ (only the 3L* case is plotted in Fig. 1). The $|\Delta E|$ are of less than half of the observed 2.5 eV[25]. On the other hand, the

Table III. The same comparison for Ge as in Table II.

	(i, j)	$E_{exp}^{(i,j)}$	3L*	3L	5L	3L+NL(d) $R_2=0.98$	4L+NL(d) $R_2=1.0$	5L+NL(d) $R_2=0.98$a.u.
Optical	$\Gamma_2^c{}'-\Gamma_{25}^v{}'$	0.99[23]	0.97	0.98	0.99	0.99	0.99	0.99
	$\Gamma_{15}^c-\Gamma_{25}^v{}'$	3.23[23]	2.95	3.31	2.99	3.24	3.22	3.19
	$L_1^c-L_3^v{}'$	2.34[23]	2.14	2.04	2.08	2.27	2.26	2.26
	$L_3^c-L_3^v{}'$	5.80[27]	4.89	5.18	5.34	5.72	5.71	5.71
	$X_1^c-X_4^v$	4.50[23]	4.16	3.94	3.94	4.37	4.35	4.34
	$L_1^c-\Gamma_{25}^v{}'$	0.84[24]	0.90	0.89	0.86	0.85	0.86	0.85
	$X_1^c-\Gamma_{25}^v{}'$	1.26§	1.33	1.27	1.32	1.29	1.28	1.29
XPS	$\Gamma_{25}^v{}'-\Gamma_1^v$	12.6±0.3[7]	12.20	12.14	11.99	12.55	12.52	12.51
	$\Gamma_{25}^v{}'-L_2^v{}'$	10.6±0.4[7]	10.23	10.15	10.11	10.47	10.46	10.45
	$\Gamma_{25}^v{}'-L_1^v$	7.7±0.2[7]	7.11	7.06	7.02	7.44	7.42	7.41
	$\Gamma_{25}^v{}'-L_3^v{}'$	1.4±0.2[23][24]	1.24	1.15	1.22	1.42	1.41	1.41
	$\Gamma_{25}^v{}'-X_4^v$	2.9±0.3¶	2.83	2.67	2.62	3.08	3.07	3.05
UPS	$L_3^c-\Gamma_{25}^v{}'$	4.3[25]	3.66	4.03	4.12	4.31	4.28	4.29
	$\Gamma_1^c-\Gamma_{25}^v{}'$	7.1[25]	8.54	7.40	7.07	6.86	6.94	6.94
	$\Gamma_{12}^c{}'-\Gamma_{25}^v{}'$	9.6[25]	7.21	7.83	8.33	9.34	9.60	9.62
		$\bar{\delta}$ (%)	9.61†	10.64	10.04	2.96	2.95	3.05
	$\Sigma_3^c-\Sigma_2^v$	4.50[23]	4.01	3.94	3.93	4.33	4.32	4.30
	$\Gamma_{25}^v{}'-\Delta_{min}^c$	1.06[30]	1.16	1.13	1.15	1.08	1.10	1.07
	$\Gamma_{25}^v{}'-\Sigma_{min}^v$	4.5±0.2[7] / 4.9[4]	3.97	3.92	3.83	4.38	4.37	4.36
	$\Gamma_{25}^v{}'-W_2^v$	3.6[4]	3.49	3.43	3.36	3.87	3.85	3.84
	$\Gamma_{25}^v{}'-W_1^v$	8.6[4]	8.99	8.30	8.30	8.58	8.57	8.57

† Value estimated by assuming that the calculated values of 7.21eV and 8.54eV correspond to the experimental values of 7.1eV and 9.6eV, respectively.

§ Value estimated from the $\Delta_{1,\,min}-\Gamma_{25}{}'=1.06$eV in ref. 30 and the experimental value $X_1-\Delta_{1,\,min}=0.2$eV of Herman, F., Kortum, R.L., Kuglin, C.D. et al.: New Studies of the Band Structure of Silicon, Germanium and Grey Tin (pp. 381-428 of ref. 31).

¶ J.E. Rowe, as cited in ref. 17.

NLEPP fittings can reproduce ΔE of 2.48~2.68 eV (Table III). The case of $\Delta E>0$ also fails in reproducing the $\Gamma_{2'}-L_1$ LS, giving only half of the observed 0.15 eV. All of these facts suggest the correct order being such that $\Delta E>0$ for both Si and Ge as shown in Fig. 2. The sign of ΔE has been undefinite experimentally[25] and theoretically[12][13]. The interpretation is supported by considering the role of the d-core repulsion (see below).

In the LEPP fittings, the increase of the number of the parameters shifts the calculated LS favorably toward the observed one. For example, in Ge, $\Delta E=0.43$ (3L), 1.03 (4L, not shown in Table III) and 1.26 (5L) eV (the observed=2.5 eV), and the $\Gamma_{12'}-\Gamma_1=0.09$ (3L), 0.12 (4L) and 0.13 (5L) eV (the observed=0.15 eV). These results, however, show that there exists a limitation in the interdependent modulation within the LEPP. As discussed above, the situation is greatly improved by the NLEPP.

As expected from the core structure, the l-

dependent nonlocality arising from the core repulsion may be of s and/or p symmetries for Si, and of d symmetry for Ge. As compared with the outermost s and p core levels of Si and Ge, the $3d$ core level of Ge lies very near the valence levels. The improvement by the NLEPP fitting is, therefore, more striking for Ge than for Si, as just seen in Table II and III.

The d-like $\Gamma_{12'}$ level of Ge lies considerably higher above the Γ_1 conduction level (2.5 eV) as compared with the case of Si (0.7 eV) (Fig. 2). The d-nonlocality of the $3d$-core repulsion can lift up the level through the d-d interaction. The $\Gamma_{12'}-\Gamma_1$ LS is acculately accounted for in the 3L+NL (d) or the 4L+NL (d) EPP, while the 5L EPP gives only the value of 1.26 eV. In Si without d core, the observed LS (0.7 eV) is well explained by the 5L EPP (0.65 eV).

An l-nonlocality corrects not only the levels specified group-theoretically by the l-symmetry, but also the other levels indirectly through the local component modulated interdependently, of course obeying the group-theory strictly. As a result, a favorable fitness of various LS's can be attained. This is the reason why, for example, the 3L+NL(s) and the 3L+NL(p) EPP's of Si show a similar fitness (Table I).

All of the above discussions do not depend on the simplified square-well model for the NLEPP. The Gaussian-well EPP optimization does not show any appreciable difference between the two types of calculation. The following EPP's of 3L+NL (p) (Si) and 3L+NL (d) (Ge) are good results in the Gaussian well model, optimized under the $\bar{\delta}$-minimization: For Si $V_L(3)=-0.2053$, $V_L(8)=0.0355$, $V_L(11)=0.0724$, $A_1=-2.8749$ (Ry/atom), $R_1=0.70$a.u. with $\bar{\delta}=3.82\%$. For Ge, $V_L(3)=-0.2406$, $V_L(8)=0.0254$, $V_L(11)=0.0522$, $A_2=-5.1988$ (Ry/atom), $R_2=1.0$ a.u. with $\bar{\delta}=3.32\%$.

The III-V or II-VI compound semiconductor with the antisymmetrical component of potential requires a doubled number of the EPP parameters as compared with the IV-group Si or Ge. The method described here will work effectively in optimizing these many parameters interdependently.

References

1) Heine, V.: The Pseudopotential Concept, Solid State Physics, ed. by Ehrenreich, H., Seitz, F. and Turnbull, D., Academic Press, New York, 1970, pp. 1-36.
2) Cohen, M.L. and Heine, V.: The Fitting of Pseudopotentials to Experimental Data and their Subsequent Application, Solid State Physics, ed. by Ehrenreich, H., Seitz, F. and Turnbull, D., Academic Press, New York, 1970, pp. 38-248
3) Cohen, M.L. and Bergstresser, T.K.: Band Structures and Pseudopotential Form Factors for Fourteen Semiconductors of the Diamond and Zinc-blende Structures, Phys. Rev., **141**, 789-796, 1966
4) Ley, L., Kowalczyk, S., Pollak, R.A. *et al.*: X-Ray Photoemission Spectra of Crystalline and Amorphous Si and Ge Valence Bands, Phys. Rev. Lett., **29**, 1088-1092, 1972
5) Pollak, R.A., Ley, L., Kowalczyk, S. *et al.*: X-Ray Photoemission Valence Band Spectra and Theoretical Valence Band Densities of States for Ge, GaAs and ZnSe, Phys. Rev. Lett., **29**, 1103-1105, 1972
6) Ley, L., Pollak, R.A., McFeely, F.R. *et al.*: Total Valence Band Densities of States of III-V and II-VI Compounds from X-Ray Photoemission Spectroscopy, Phys. Rev., **B9**, 600-621, 1974
7) Grobman, W.D. and Eastman, D.E.: Photoemission Valence Band Densities of States for Si, Ge and GaAs Using Synchrotron Radiation, Phys. Rev. Lett., **29**, 1508-1512, 1972
8) Eastman, D.E., Grobman, W.D., Freeouf, J.L. *et al.*: Photoemission Spectroscopy using Synchrotron Radiation. I. Overviews of

Valence-Band Structure for Ge, GaAs, GaP, InSb, ZnSe, CdTe and AgI, Phys. Rev., **B9**, 3473-3488, 1974

9) Aspnes, D.E.: Linearized Third-Derivative Spectroscopy with Depletion-Barrier Modulation, Phys. Rev. Lett., **28**, 913-916, 1972

10) Aspnes, D.E. and Rowe, J.E.: E_1 Transition in Ge — Two Dimensional or Three Dimensional?, Phys. Rev., **B7**, 887-891, 1973

11) Aspnes, D.E. and Studna, A.A.: Schottky-Barrier Electroreflectance — Application to GaAs, Phys. Rev., **B7**, 4605-4625, 1973

12) Chelikowsky, J.R. and Cohen, M.L.: Nonlocal Pseudopotential Calculations for the Electronic Structure of Eleven Diamond and Zinc-blende Semiconductors, Phys. Rev., **B14**, 556-582, 1976

13) Chelikowsky, J.R. and Cohen, M.L.: Electronic Structure of Silicon, Phys. Rev., **B10**, 5095-5107, 1974

14) Chelikowsky, J.R., Chadi, D.J. and Cohen, M.L.: Calculated Valence Band Densities of States and Photoemission Spectra of Diamond and Zinc-blende Semiconductors, Phys. Rev., **B8**, 2786-2794, 1973

15) Chelikowsky, J.R. and Cohen, M.L.: High Resolution Band Structure and the E_2 Peak in Ge, Phys. Rev. Lett., **31**, 1582-1585, 1973

16) Chelikowsky, J.R. and Cohen, M.L.: Electronic Structure of GaAs, Phys. Rev. Lett., **32**, 674-677, 1974

17) Phillips, J.C. and Pandey, K.C.: Nonlocal Pseudopotential for Ge, Phys. Rev. Lett., **30**, 787-790, 1973

18) Pandey, K.C. and Phillips, J.C.: Nonlocal Pseudopotentials for Ge and GaAs, Phys. Rev., **B9**, 1552-1559, 1974

19) Abarenkov, I and Heine, V.: The Model Potential for Positive Ions, Phil. Mag., **12**, 529-537, 1965

20) Kane, E.O.: Band Structure of Silicon from an Adjusted Heine-Abarenkov Calculation, Phys. Rev., **146**, 558-567, 1966

21) Nara, H. and Kobayasi, T.: Nonlocal Pseudopotentials of Si and Ge, J. Phys. Soc. Jpn., **41**, 1429-1430, 1976

22) Nara, H. and Schlesinger, M.: Analysis of the Optical Spectra of Dy^{3+} Doped Calcium Fluoride, J. Phys. C-Solid State Phys., **5**, 606-614, 1972

23) Aspnes. D.E.: Interband Masses of Higher Interband Critical Points in Ge, Phys. Rev. Lett., **31**, 230-233, 1973

24) Fischer, J.E.: Transverse Electroreflectance and the Band Structure of Germanium, Proceedings of the 10th International Conference on the Physics of Semiconductors, USAEC, Ork Ridge, USA, 1970, pp. 427-432

25) Spicer, W.E. and Eden, R.C.: Photoemission Investigation of the Band Structure of Semiconductors, Proceedings of the 9th International Conference on the Physics of Semiconductors, Nauka, Leningrad, USSR, 1968, vol. **1**, pp. 65-92

26) Aspnes, D.E. and Studna, A.A.: Direct Observation of the E_0 and $E_0+\Delta_0$ Transitions in Si, Solid State Commun., **11**, 1375-1378, 1972

27) Zucca, R.R.Z. and Shen, Y.R.: Wavelength-Modulation Spectra of Some Semiconductors, Phys. Rev., **B1**, 2668-2676, 1970

28) Frova, A. and Handler, P.: Direct Observation of Phonons in Silicon by Electric-Field-Modulated Optical Absorption, Phys. Rev. Lett., **14**, 178-180, 1965

29) Seraphin, B.O.: Optical Field Effect in Silicon, Phys. Rev., **140**, A1716-A1725, 1965

30) Braunstein, R., Moore, A.R. and Herman, F.: Intrinsic Optical Absorption in Germanium-Silicon Alloys, Phys. Rev., **109**, 695-710, 1958

31) Quantum Theory of Atoms, Molecules and Solid State, ed. by P.O. Löwdin, Academic Press, New York, 1966